CORRELATION BETWEEN X-RAY FLUX AND ROTATIONAL ACCELERATION IN VELA X-1

J. E. Deeter and P. E. Boynton[1]
Department of Astronomy, University of Washington

N. Shibazaki
Department of Physics, Rikkyo University

S. Hayakawa
Department of Astrophysics, Nagoya University

and

F. Nagase
Institute of Space and Astronautical Science

Final Technical Report
NASA Grant NAGW 1133
February 1989

This Final Technical Report is presented to NASA with the understanding that the scientific results contained herein are preliminary and are not in their present form intended for publication or citation.

[1] Also Department of Physics, University of Washington.

ABSTRACT

We present the results of a search for correlations between X-ray flux and angular acceleration for the accreting binary pulsar Vela X-1, based on data obtained with the Hakucho satellite during the interval 1982-1984. In undertaking this correlation analysis, we found it necessary to modify the usual statistical method to deal with conditions imposed by generally unavoidable satellite observing constraints, most notably a mismatch in sampling between the two variables. Our results are suggestive of a correlation between flux and the absolute value of the angular acceleration, at a significance level of 96 percent. We discuss the implications of the methods and results presented here for future observations and analysis.

Subject headings: stars: neutron---stars: rotation---X-rays: binaries---pulsars---numerical methods

I. INTRODUCTION

Variations in the rotation rate of X-ray pulsars are an inevitable consequence of matter accretion. Theoretical studies indicate that a description of accretion torques must take into account not only the mass accretion rate, but the accretion flow pattern as well as the role of the neutron star magnetosphere (Lamb 1989, and references therein). Observations of the variation in rotation rate for several accretion-powered pulsars have provided significant constraints on these models (Boynton et al. 1984; Nagase et al. 1984; Deeter et al. 1989). However, a more detailed probing of accretion physics is possible by simultaneously observing both the neutron star angular acceleration, α, and the X-ray flux, F, the two principal manifestations of the accretion process. According to preliminary theoretical studies and simulations reported by Lamb (1985), the character of the temporal correlations between F and α is distinctly dependent on whether the accretion flow is radial or disk-mediated, and whether the system can be described as a fast or a slow rotator.

Despite the attractiveness of investigating correlations between F and α as a tool for understanding accretion flows, only one observational study has previously been reported, for the transient X-ray source EXO 2030+375 (Parmar et al. 1988). This is partly because of difficulty in obtaining adequate observations. For most pulsars, the angular acceleration is much smaller than its uncertainty for intervals shorter than a few days and it therefore takes a demanding observing program to obtain even a small number of independent (F, α) pairs. But even with an adequate data base, correctly accounting for the fundamental disparity in the way that F and α are sampled requires the development of an extention of the customary statistical methods for analyzing and interpreting the correlations between these variables.

This paper consequently has two purposes: to explicate and modify the customary mathematical and statistical tools necessary to undertake a determination of the correlation between flux and angular acceleration, and then to apply the resulting procedures to the Hakucho observations of the accretion-powered pulsar Vela X-1. The result of this analysis

suggests a possible correlation between F and α , but this result is by no means definitive. However, as a consequence of developing a method of analysis, we are able to indicate conditions for future observations of other sources that should provide a more favorable opportunity to study accretion physics through F-α correlations.

In § II we briefly review a simple statistical model based on the physics relating X-ray flux and neutron star angular acceleration . In § III we outline the method of analysis used in the correlation study, leaving details for a series of Appendices. In § IV we discuss available data sets and our choice for the analysis in this paper. In § V we present the results of our study of the Hakucho data on Vela X-1. In § VI we discuss the implications of these results for future observations and analysis.

II. FOUNDATIONS FOR A STATISTICAL MODEL

In the conventional interpretation, an X-ray pulsar is a rotating neutron star whose luminosity arises from mass accretion. Because the accreted material carries angular momentum, there will be an accretion torque and consequently changes in the rotation rate of the neutron star. There is sufficient theoretical understanding of the resulting correlation between mass accretion rate and the accretion torque to distinguish between various types of accretion flows (Lamb 1985; Lamb et al. 1989).

What makes F and α the appropriate choice of observables for studying the physics of accretion? The physical models proposed by Ghosh and Lamb (1978, 1979a,b) can all be expressed as relations between the mass accretion rate $\dot{M}$ and the torque N acting on the neutron star. Under rather mild assumptions, these can be restated as relations between the more directly observable variables F and α. In particular, the star must be sufficiently rigid so that internal torques are unimportant and thus $\alpha = N/I_S$, where I_S is the moment of inertia of the neutron star. On the other hand, the X-ray flux must be a good indicator of the mass accretion rate (no beam wandering, no variable absorption, no delayed nuclear burning of accreted material). Under these conditions, the α-F

relation is identical up to a multiplicative constant to the N-$\dot{M}$ relation. This relationship can be established for a particular source provided the accretion rate is sufficiently variable to allow sampling of a reasonable range of both F and α.

In fact, we observe the angular acceleration of the neutron star rotation indirectly, identifying it with the time derivative of the X-ray pulse frequency. This identification may be comprimised by pulse shape noise and by wandering of the X-ray beam pattern. We discuss both of these issues later in this section, justifying the naive point of view that pulse frequency is identical to rotation frequency, and that the measured frequency differs from both only because of uncertainties introduced by pulse shape noise. This convention allows us to keep the notation simple, using α(t) to denote the time history of the angular acceleration of the neutron star rotation, and $\hat{\alpha}$ (or a similar modification of α) for the measured derivative of the pulse frequency averaged over some specified interval. Thus, in the remainder of this paper, α will formally represent the derivative of the pulse frequency (the observed variable), which we interpret whenever necessary as the angular acceleration of the neutron star rotation.

Except for the transient source EXO 2030+375 (Parmar et al. 1988), direct observational evidence for a relationship between F and α is presently rather weak for any X-ray pulsar, but there is substantial indirect evidence that these correlations could be present in Vela X-1. For instance, both flux and angular acceleration exhibit large fluctuations, and the noise properties of the two variables are strikingly similar. This similarity is virtually a sine qua non for the existence of correlations, since any two correlated variables should have nearly identical noise properties. In the following discussion of the fluctuations in F and α, we concentrate on comparing the similaries in their power density spectra.

Vela X-1 exhibits large variations in angular acceleration with spindown and spinup observed on a wide range of timescales (Nagase et al. 1984; Boynton et al. 1984; Deeter et al. 1989). The power density spectrum of α has been previously discussed by Boynton et al. (1984) and

Deeter et al.(1987, 1989), who show that it is nearly flat for analysis frequencies between 0.0003 and 0.2 d^{-1}, and follows approximately an f^4 power law for higher frequencies. The interpretion of the spectrum of α as a superposition of two distinct noise processes having spectra described by two different power laws (Deeter et al. 1989) is a crucial ingredient in a comparision with the spectrum for F . At analysis frequencies below 0.2 d^{-1} the power density spectrum for α is dominated by variations in the rotation rate of the neutron star, and this portion of the spectrum is flat (f^0 power law) within the uncertainty in determining the power-law exponent. For analysis frequencies above the crossover frequency 0.2 d^{-1}, a separate process with an f^4 power law dominates the spectrum. We understand this second component as arising from fluctuations in pulse shape, inducing fluctuations in the measured pulse phase, frequency, and angular acceleration. The division of the power density spectrum of the variations in α into two regimes is particularly appealing because of the simplicity of explaining the two different power laws in the low and high frequency regimes in terms of distinct processes.

There are, however, possible ambiguities in this simple interpretation of the spectrum, particularly at analysis frequencies in the vicinity of the transition between the two power laws. For instance, van der Klis and Bonnet-Bidaud (1984) have suggested that part of the variations at lower analysis frequencies might be due to changes in the direction of the pulsar beam pattern rather than true variations in the rotation rate of the neutron star. This explanation can be ruled out at analysis frequencies lower than 0.01 d^{-1}, for which the inferred phase excursions become larger than π radians (Deeter et al. 1989). It is therefore almost certain that the fluctuations at the lowest frequencies are due to variations in the rotation rate of the crust of the neutron star. At frequencies between 0.01 and 0.2 d^{-1}, however, a substantial fraction of the power density could be due to beam wandering. In this region the spectrum of α is still nearly flat, and any power density arising from beam wandering must be somewhat compensated by a corresponding decrease in the power density from fluctuations in the rotation rate. Even though there is a degree of articifiality in proposing a third component in the fluctuations of the

measured angular acceleration, further evidence is required to rule out this case altogether.

To strengthen the argument against a third component in the spectrum of the fluctuations in α, we consider what observable effect beam wandering would have on the pulse shape. In the simplest case of a beam with a fairly narrow, two-dimensional gaussian profile, no change in pulse shape would result from wandering in azimuth and only a change in amplitude would result from wandering in elevation, where azimuth and elevation refer to a fixed coordinate system centered on the neutron star. This simple behavior clearly does not apply for pulsations with complex waveforms, such as seen in Vela X-1, for which it is difficult to have beam wandering without a concomitant change in pulse shape. In particular, changes in pulse shape entail changes in the relative phases of the pulse harmonics, and we can directly compare the fluctuations in these harmonic phase differences to the fluctuations in overall pulse phase. Thus, in Figure 1, we show the variation with time of the pulse phase of Vela X-1 for a subset of the Hakucho data, together with the phases of the individual harmonic components relative to a smooth trend obtained by fitting a quadratic function in time to the variation in pulse phase. In this figure, the first harmonic has been omitted, because its amplitude is close to zero, and the phase of the third harmonic is relatively noisy as its amplitude is small. The remaining harmonic phases track each other quite well for time scales longer than about 2 days (corresponding to analysis frequencies lower than 0.08 d^{-1}), indicating no appreciable change in pulse shape despite large changes in pulse phase over this same time interval.[2] This largely closes the frequency gap within which beam

---

[2] There are hints of very small secular variations in the differential phases, but these are at least an order of magnitude smaller than the change in overall pulse phase.

---

wandering can contribute to the power density spectrum of the phase (and angular acceleration) fluctuations.

We turn now to variations in the X-ray flux, for which fluctuations of a factor of five are obseved on a timescale of hours (Nagase et al. 1984).

Using the method presented in Appendix A, we constructed a power density spectrum of the flux for analysis frequencies between 0.001 and 4 d^{-1}, based on data obtained with Hakucho. This spectrum, shown in Figure 2, is virtually flat for analysis frequencies between 0.001 and 0.3 d^{-1}. In contrast to α, all variations in the flux, such as those due to the finite number of photons detected, are likely to have a flat power density spectrum. Thus, the characteristic crossover frequency observed in the spectrum of the fluctuations in α is not present in the corresponding spectrum for F. The decrease in power density at the higher frequencies is in agreement with the nature of the variations seen in the time history, wherein the fluctuations are relatively smooth on time scales smaller than one or two hours (Nagase et al. 1984).

The power density spectra of the fluctuations in F and α are very similar within their common range of analysis frequencies from 0.001 to 0.2 d^{-1}. Above the crossover frequency 0.2 d^{-1}, where fluctuations in the rotation rate of the neutron star are obscured by pulse shape noise, we cannot directly compare the two spectra. Thus we cannot discern whether the spectrum of the rotational angular acceleration decreases above 0.3 d^{-1} as does the spectrum of F.

The similarity of the two power density spectra is a precondition for a strong correlation between F and α, but of course does not by itself establish the existence of a correlation. To determine whether or not a correlation is present in a particular data set requires the use of a statistical correlation analysis technique. Even so, the power density spectra provide information that is helpful in undertaking and interpreting the correlation analysis. For instance, the drop in flux power density at frequencies above 0.3 d^{-1} , indicating that the flux variations are smooth on timescales shorter than a few hours, but that they undergo large excursion on longer timescales. On the other hand, determinations of α on single intervals shorter than 3 or 4 days are dominated by noise from variations in pulse shape, and are therefore useless for a correlation diagram. To get correlation pairs (F, α) with a meaningful estimate for α, we for shorter intervals we must average over many separate excursions in the mass accretion rate.

Averaging does not wash out any approximately linear relationship between the two variables, but the magnitude of the variations will likely decrease as the averaging time scale is lengthened. However, averaging over many independent "events" (separate excursions in the mass accretion rate) suggests a statistical approach to analyzing the flux and angular acceleration for correlations. In § III we develop suitable technique, showing how to modify a common statistical treatment to deal with the several complications inherent to these data.

III. METHODOLOGY

a) Statistic for the Correlation Coefficient

For simple accretion-torque models, variations in X-ray flux and in the rotational acceleration are both correlated with variations in mass accretion, and hence with each other. We observe that variations in F and α separately have the character of white noise, with a possible high-frequency cut-off set by the duration of an individual accretion event. Averages of F and α over an interval whose length T is larger than the duration of accretion events have variances which scale inversely with T,

$$\tau_F^2(T) = \langle \Delta F_T^2 \rangle = S_F/T\,, \tag{1a}$$

$$\tau_\alpha^2(T) = \langle \Delta \alpha_T^2 \rangle = S_\alpha/T\,. \tag{1b}$$

Here S_F and S_α represent the white noise strength for the variations in the X-ray flux F and the angular acceleration α. (The rms variations caused by fluctuations in the accretion process are denoted by τ_F and τ_α, reserving σ to represent other noise contributions such as those due to finite count rates.) Motivated by simple accretion models, we assume that concurrently sampled F_T and α_T are correlated,

$$\mathrm{cov}(F_T, \alpha_T) = \rho \tau_F(T) \tau_\alpha(T)\,, \tag{2}$$

with the correlation coefficient ρ close to unity, and that the correlation coefficient does not depend on the averaging time scale T.

Under ideal observing conditions of continuous sampling of F and α, the correlation between these variables can be estimated in a straightforward manner. The data are divided into a series of disjoint subintervals, each of length T, and concurrent averages F_k and α_k are computed for the kth subinterval. Mean values ($\bar{F}$, $\bar{\alpha}$) and rms variations ($\hat{\tau}_F$, $\hat{\tau}_\alpha$) are estimated for the two variables F and α, and the sample correlation coefficient is computed using the statistic,

$$\hat{r} = \frac{1/n \sum_{k=1}^{n} (F_k - \bar{F})(\alpha_k - \bar{\alpha})}{\hat{\tau}_F \hat{\tau}_\alpha} . \qquad (3)$$

The distribution of this statistic is relatively simple, giving a ready estimate of its uncertainty and providing a test for the significance of a nonzero value.

A complication in applying this statistic to actual data is the presence of noise components in F and α in excess of the variations linked directly to the mass accretion process. We will denote the rms size of these excess noise components by σ_F and σ_α, so that the total variances in the two variables are given by,

$$\text{var } F = \tau_F'^2 = \tau_F^2 + \sigma_F^2 , \qquad (4\underline{a})$$

$$\text{var } \alpha = \tau_\alpha'^2 = \tau_\alpha^2 + \sigma_\alpha^2 . \qquad (4\underline{b})$$

To make the notation less cumbersome, explicit indication of the averaging time scale has been suppressed.

As discussed by Boynton et al. (1986) and Boynton and Deeter (1986), an excess noise component in the angular acceleration arises from fluctuations in pulse shape that induce white noise in pulse phase. For data sampled uniformly in time, the uncertainty in α from this noise component scales as $T^{-5/2}$, where T is the length of the analysis interval. On the other hand, the fluctuations in α arising from accretion torques are observed to have the character of white noise, for which the rms variation in α scales as $T^{-1/2}$ (Deeter et al. 1987, 1989). On short timescales, the uncertainty in α due to noise in pulse shape therefore dominates the torque variations. This situation is described by Boynton

et al. (1986) in terms of a crossover frequency in the power spectrum of variations in α, where the power law exponent is seen to change from zero to almost four -- equivalent to the change of two in the exponent of the scaling laws for the rms variation described above.

An important consequence of this crossover frequency (or crossover timescale) is that it restricts the averaging time appropriate for computing correlations. In particular, estimates of the angular acceleration on short time scales will be dominated by variations due to pulse-shape noise, and the correlation between F and α arising from mass accretion will be hopelessly obscured. This situation, wherein the excess noise increases rapidly at short time scales, can be compared to the case in which all sources of noise are approximately white and the rms variation scales as $T^{-1/2}$ on all time scales. If this were true for both variables being correlated, then the correlation analysis could be undertaken on as short a timescale as practical, thus maximizing the number of correlation pairs. This freedom is lost in the present situation where the pulse-shape noise increases so rapidly with decreasing timescale, that it eventually dominates all other noise processes.

Local values of the angular acceleration are obtained from analyzing the pulse phases, which constitute an available intermediate data record. We want to choose an method of estimating α which minimizes the ratio of the contribution from pulse shape noise to the contribution from fluctuations in the accretion torque. For example, in the case of constant acceleration, the contribution from pulse shape noise is minimized when the angular acceleration is estimated by the quadratic coefficient α_o from a second-degree least-squares fit to the phase,

$$\phi(t) = \phi_o + \Omega_o (t - t_o) + \frac{\alpha_o}{2} (t - t_o)^2 , \qquad (5)$$

where the coefficients ϕ_o and Ω_o (the phase and frequency at time t_o) are also parameters in the least-squares solution. However, our model differs in that the actual acceleration is not constant but is characterized by white noise. In this case, the estimate of angular acceleration which achieves the greatest response to the actual acceleration with the least

response to pulse shape noise is the "lowest-mode estimator" discussed by Deeter and Boynton (1982). Using the methods of that paper, it can be shown that the estimate provided by the quadratic coefficient has an efficiency of 98% -- that is, its variance is only 2% larger than that of the lowest-mode estimator. The determination of the lowest-mode estimator requires solving an eigenvalue problem, a procedure which is considerably more complex than the computation of the quadratic coefficient. In the interest of simplicity we therefore accept the latter as a practical alternative to the exact solution of the noise minimization problem.

Having adopted the quadratic coefficient α_o as a simple and efficient local estimator of α, we next must assure that the estimates of F and α from an interval [a, b] are truly concurrent. This issue is treated in Appendix B, where we show that the estimate α_o can be expressed as a sampling function $\hat{g}(t)$ applied to pulse phase,

$$\alpha_o = \int_a^b \hat{g}(t)\phi(t)\, dt\,, \tag{6}$$

and that this integral can be rewritten using integration by parts to exhibit explicitly the equivalent sampling of angular acceleration,

$$\alpha_o = \int_a^b \hat{g}^{(-2)}(t)\alpha(t)\, dt\,. \tag{7}$$

The function $\hat{g}^{(-2)}(t)$ is the particular second integral of $\hat{g}(t)$ which vanishes at the end points (a, b), and is strictly continuous. On the other hand, $\hat{g}(t)$ can be highly discontinuous, jumping to zero wherever data is missing. Thus each local estimate of α from the quadratic coefficient is a continuous average of the entire run of $\alpha(t)$ in the interval, even if the flux and hence pulse phase are sampled discontinuously.

The data set analyzed in this paper is quite discontinuous, as the the sampling is affected by Earth occultations, satellite operations, and other interruptions. Thus the average X-ray flux for a given interval is based on data from a subset consisting of many subintervals separated by significant gaps. The closest match for a flux average to the estimate

of α (eqn. 7) is obtained by applying the sampling function $\hat{g}^{-2}(t)$ to the flux data on the subset of observations as indicated in Appendix C by equation (C3). Thus the sampling of the two variables is not strictly concurrent; that is, there is a "mismatch" in sampling. In Appendix C we show that this mismatch leads to a dilution of the observed correlation coefficient with respect to the "true" correlation for concurrent sampling, even in the absence of excess noise in F and α. Indeed, any uncorrelated noise in either variable will further dilute the observed correlation. The diluted correlation coefficient ρ' is given by the expression,

$$\rho' = \frac{\mathrm{cov}(F, \alpha)}{(\mathrm{var}\, F\, \mathrm{var}\, \alpha)^{1/2}} = x' \frac{\tau_F}{\tau_F'} \frac{\tau_\alpha}{\tau_\alpha'} \rho , \tag{8}$$

where the factor x' accounts for dilution due to incomplete sampling of F (see eq. [C11] in Appendix C) and the remaining factors account for dilution from excess noise (cf. eqs. [4a,b], and eq. [C13]).

A final complication arises from irregularities in the data sampling that cause the dilution to differ among the various sample pairs (F_k, α_k). To combine the correlation pairs within a single analysis requires that they be assigned weights in the computation. In Appendix D, we show that these weights should be proportional to the dilution $y_k = x_k' [\tau_F/\tau_F'] [\tau_\alpha/\tau_\alpha']$, and that a reasonable statistic for the correlation coefficient is

$$r^\dagger = \sum_{k=1}^{n} y_k \frac{(F_k - \bar{F})(\alpha_k - \bar{\alpha})}{\tau_F' \tau_\alpha'} \Big/ \sum_{k=1}^{n} y_k . \tag{9}$$

The expectation and variance of $r^\dagger$ are

$$E(r^\dagger) = \rho \sum_k y_k \Big/ \sum_k y_k^2 , \qquad \text{and} \tag{10a}$$

$$\mathrm{var}\, r^\dagger = \Big[\sum_k y_k \Big] \Big/ \sum_k y_k^2 , \tag{10b}$$

in the limit that the diluted correlation $y_k \rho$ is small for each summand (cf. eqs. [D8] and [D9] in Appendix D). The variance of $r^\dagger$ is necessary

later on for determining the uncertainty in the estimated correlation coefficient and for evaluating the significance of a nonzero value.

b) Determination of Noise Strengths for F and α

The determination of the white noise strengths S_F and S_α (see eq. 1a,b) and the average values $\bar{F}$ and $\bar{\alpha}$ have not yet been specified. The noise strengths correspond to the variances $\hat{\tau}_F^2$ and $\hat{\tau}_\alpha^2$ for the case of computing the correlation coefficient on homogeneous data (cf. eq. 2), and are usually computed directly from the actual scatter in the two variables.

The case of X-ray flux is relatively straightforward, since fluctuations in addition to those contributed by the mass accretion process have similar noise properties. For the data we analyze, this additional noise component is negligible compared to the variations from mass accretion (cf. Appendix A), and an exact treatment is not necessary. We therefore absorb the additional noise component into the overall noise strength S_F. With this simplification, the variance for the kth interval scales inversely with the effective duration of the interval over which the flux is averaged, T'_k,

$$\tau'^2_{F,k} = S_F / T'_k \,. \tag{11}$$

Thus a reasonable estimate for S_F is given by

$$S_F = \frac{1}{n} \sum_k T'_k (F_k - \bar{F})^2 \,, \tag{12}$$

with a compatible estimate of $\bar{F}$ given by a weighted average of the individual F_k,

$$\bar{F} = \sum_k T'_k F_k \Big/ \sum_k T'_k \,. \tag{13}$$

What complicates the computation in the case of the angular acceleration, α is the presence of a second noise source with distinctly different properties (white noise on ϕ rather than α). The contributions to the variance of each estimate α_k from pulse shape variations and from

fluctuations in mass accretion are comparable in magnitude for averages over intervals whose durations are close to crossover timescale, and so the pulse shape variations cannot be ignored. We could obtain an estimate of S_α by subtracting the pulse-shape contribution to the variances of the α_k. In practice, this "subtraction" is accomplished by choosing that value of S_α for which the observed scatter just matches the expected scatter in the α_k,

$$\sum_k \frac{(\alpha_k - \bar{\alpha})^2}{T_k \tau'^4_{\alpha,k}} = \sum_k \frac{1}{T_k \tau'^2_{\alpha,k}}, \tag{14}$$

This particular method of weighting is obtained from the maximum likelihood criterion applied to S_α.[3] The average value of the angular acceleration $\bar{\alpha}$

[3] For a discussion of maximum likelihood estimates, see Lindgren 1962. The divisor T_k and the extra factor $\tau'^2_{\alpha,k}$ in the denominators in equation (14) effectively reduce the importance of points with relatively large observational errors compared to intrinsic scatter.

is specified by the equation

$$\bar{\alpha} = \sum_k \frac{\alpha_k}{\tau'^2_{\alpha,k}} \Big/ \sum_k \frac{1}{\tau'^2_{\alpha,k}}. \tag{15}$$

Equations (14) and (15) constitute a non-linear problem in two unknowns, $\bar{\alpha}$ and S_α, that may be solved by a Newton-type method starting with $S_\alpha = 0$. Note that if the actual scatter is already less than the estimated observational errors, this procedure would give a negative value for S_α, and therefore the contribution from intrinsic noise would be negligible. For each of the correlation sets presented here the observed scatter was in fact larger than that predicted from the observational uncertainties.

In this section, we have shown that a mismatch in sampling between X-ray flux and pulse angular acceleration causes the measured correlation between them to be smaller in magnitude than the actual correlation. In addition, we have shown how to handle inhomogeneous data having different reductions for the various (F, α) pairs, by modifying the formula for the correlation coefficient to weight the pairs in proportion to their

dilutions. In any event, the reduction in the correlation coefficent must be taken into account in assessing the results of the correlation analysis.

IV. CHOICE OF DATA SET FOR ANALYSIS

The procedure outlined in § III for computing the correlation between X-ray flux and angular acceleration imposes some fairly severe restrictions on the character of data suitable for analysis. The X-ray flux and the angular acceleration should both have noticeable variations ascribable to the mass accretion process. Specifically, variations in the flux should be considerable larger than those due to counting statistics, and the X-ray flux should be sampled as completely as possible to minimize dilution of the observed correlation. Even though variations in angular acceleration due to mass accretion are expected to dominate variations induced by fluctuations in pulse shape on sufficiently long timescales, it is desirable that this timescale be as short as possible in order to obtain the largest possible number of correlation pairs. Finally, it is useful that the X-ray flux be observed in two or more energy channels, so that the effect of variable absorption can be assessed and removed. In particular, two energy channels, one above and one below a nominal 10 keV, are the minimal requirement to monitor variable absorption.

Up to now, no data seem to have been obtained specifically for the purpose of studying F-α correlations. Furthermore, most of the existing data sets on X-ray pulsars are clearly not suitable for this purpose. Early data sets, such as the extensive observations of Her X-1 and Cen X-3 by Uhuru, have low counting rates and uncertain collimator corrections, resulting in poorly determined X-ray fluxes and long crossover timescales . Later data sets from satellites with large detector area (such as HEAO 1) were often limited to a day's duration and were therefore too short to provide a useful number of correlation pairs.

A promising X-ray source for studying F-α correlations from existing data is Vela X-1. Not only does this source exhibit large variations in both flux and angular acceleration, but it has also been observed extensively during the past ten years. These observations include

four fairly large sets: (1) OSO 8 in 1978 May; (2) HEAO 1 in 1978 November--December; (3) Hakucho in 1980--1982; and (4) Tenma in 1983 March and 1984 March. We will briefly discuss the merits and liabilities of these sets as concrete illustrations of the problems of designing or selecting a data set with favorable properties for an F-α study. For more detailed discussions of these data sets see Nagase et al. (1984), Boynton et al. (1986), and Deeter et al. (1987).

(1) The 1978 May set, obtained with OSO 8, spans about 35 days and is characterized by a particularly high data recovery fraction of about 75%. However, α is well-determined only on intervals longer than 6 days, and after excluding eclipses there are only four correlation pairs available. Only one energy channel is available, and so there is no way of correcting for variable absorption.

(2) The 1978 November--December data set (HEAO 1) consists of twelve half-day pointings over a span of 36 days, arranged in a hierarchical pattern with spacings from 1.5 days to 12 days. Determinations of α statistically different from zero are available on the relatively short interval of three days (coincidently the interval spanning three consecutive pointings at the 1.5-day spacing). Only two independent correlation pairs can be calculated on the three-day interval, with a data recovery rate of about 30%. Separate high and low energy fluxes are available.

(3) The 1980--1982 set (Hakucho) covers about 110 days in seven major blocks. Determinations of α are available on intervals longer than about 4 days, with a data recovery rate of $\sim$40%. There are between 10 and 20 independent correlation pairs, depending on the choice of interval length. Both high and low energy fluxes are available. This data set is our choice for analysis.

(4) Observations with Tenma cover a total of 10 days in 1982 March and 1983 March. Accurate determinations of α can be obtained for intervals longer than three days, with a data recovery rate of $\sim$40%. There are three independent correlation pairs, using intervals of three days duration. Multichannel energy fluxes are available.

The single data set with the best properties is the Hakucho set, primarily because it affords the largest number of independent correlation pairs. As indicated above, we have to use intervals of length greater than four days in order to obtain sufficiently precise estimates of the α arising from fluctuations in rotation. Estimates of α on shorter intervals are dominated by pulse shape noise, thereby obscuring any actual correlation with the X-ray flux. On the other hand, the loss of nearly three days due to X-ray eclipse during each 8.9-day orbital cycle restricts the correlation analysis to intervals less than the six-day span between consecutive eclipses. Bridging eclipses causes unacceptable reductions in the data recovery rate, unless two consecutive orbits can be covered within a single interval. However, there are only four independent correlation pairs with the required interval length of 15 days, and this is too small a number on which to consider a correlation analysis.

From these considerations, the time scales chosen for examination were 6 and 4 days, represented by 11 and 17 correlation pairs, respectively.

V. PRESENTATION OF COMPUTATIONS

The observations of Vela X-1 obtained with Hakucho have previously been studied by Nagase et al. (1982, 1984) and by Deeter et al. (1987). These investigations provide the initial steps in converting the raw counts to a form suitable for the present study of F-α correlations. In particular, we use the fluxes corrected for collimator shadowing determined by Nagase et al. (1984), and the pulse phases computed by Deeter et al. (1987). These reduced data require some further manipulations to covert them into F-α sample pairs.

As explained at the end of § IV, we are constrained to test for correlations using an interval length between four and six days, and decided on the two extremes. The six-day intervals are entirely disjoint, but we allowed up to one day overlap for the four-day intervals, squeezing in wherever possible two intervals between consecutive X-ray eclipses. All of these intervals are listed in Table 1.

Although the fluxes and pulse phases were computed independently, they generally matched in time, with very few satellite orbits having data from one category and not the other. One criterion in selecting an interval for analysis was that both flux and phase data were both well distributed within the interval. In §§ Va and Vb we explain how these data were converted into estimates of the local flux and angular acceleration for each interval, and in § Vc we present the computation of the correlation coefficient and tests for significance of a nonzero value.

a) Computation of Angular Acceleration

The analysis of the Hakucho data by Deeter et al. (1987) provides residual pulse phases relative to chosen reference pulse frequencies. These phases have been corrected to the inertial frame of the mean orbit for Vela X-1 reported in that paper. In principle, the residual phases could be converted to phases by adding back in the phase accumulated at the rate specified by the reference frequency. In practice, this step is unnecessary, since the addition or subtraction of a constant rate does not affect the second derivative (or quadratic term) associated with the angular acceleration. The average angular acceration α_k for the kth interval was obtained by fitting the residual pulse phases $\Delta\phi_{k,j}$ lying within the interval by a second-degree polynomial in time,

$$\Delta\phi(t) = \Delta\phi_k + \Delta\Omega_k(t - t_k) + \frac{1}{2}\alpha_k(t - t_k)^2 , \tag{16}$$

with a separate fit performed on the phase data in each interval. The parameters $\Delta\phi_k$ and $\Delta\Omega_k$ are the residual pulse phase and frequency at the midtime t_k (the value of α_k determined from a second-degree fit is actually independent of the choice of t_k). The parameters $\Delta\phi_k$, $\Delta\Omega_k$, and α are obtained by minimizing the sum of squared residuals between the observed and calculated phases in the k interval,

$$SSQ = \sum_j \left[\Delta\phi_{k,j} - \Delta\phi(t_{k,j})\right]^2 / \sigma^2_{k,j} , \tag{16a}$$

weighting the phases by their inverse variances, $\sigma^2_{k,j}$. These variances were determined from the scatter about local linear fits to the phase

data on intervals shorter than 1.6 days, and are reasonable estimates of the uncertainty induced from pulse shape noise (Deeter et al. 1987). The least-squares solution which determines α_k provides an estimate of the uncertainty in this quantity, also based on pulse shape noise. The values thus obtained for the α_k and the associated errors are listed in Table 1.

The solution to the least-squares problem provides an explicit expression for the coefficent α_k in terms of the data $\Delta\phi_{k,j}$,

$$\alpha_k = \sum_j \hat{g}_{k,j} \Delta\phi_{k,j} \cdot \tag{17}$$

For mathematical convenience, we transform this sum into an integral by introducing a function $\hat{g}(t)$ consisting of δ-functions,

$$\hat{g}(t) = \sum_j \hat{g}_{k,j} \delta(t - t_{k,j}) \cdot \tag{18}$$

This function is used below in constructing the flux estimate F_k corresponding to α_k.

The mean $\bar{\alpha}$ and the estimate of the noise strength S_α (in excess of the noise attributable to pulse-shape noise) were then computed from the individual a_k, using the method of § IIIb, and the resulting values are reported in Table 2.

b) Computation of Average X-ray Flux

The Hakucho flux data comprises two energy channels, 1--9 keV and 9--22 keV. There are obvious, strong variations in both channels at all time scales greater than a few hours (cf. Appendix A). These variations can be characterized as white noise with a high-frequency cutoff. In addition, both energy channels show systematic variations at the orbital frequency, which are stronger in the low energy channel. Detailed analysis indicates that these orbital variations are partly due to cold-matter absorption (Nagase et al. 1984), and the remainder are presumably real luminosity variations.

For use in the F-α analysis, the flux variations due to absorption should be removed. However, for the high energy channel, the absorption variations are less than 10% compared to total variations of more than a factor of five, and therefore need not be removed if only the high energy channel data are used in the analysis. There is, in addition, the possibility that systematic luminosity variations at the orbital frequency ought to be removed as well. This is because systematic variations in the angular acceleration at the orbital frequency (and its second harmonic) are removed in the orbital analysis, which relies on variations at just these frequencies to determine the orbital parameters (see e.g., Deeter, Boynton and Pravdo 1981). The exact relationship between the orbital variations in the flux and angular acceleration are, however, model dependent. For instance, if the angular acceleration reverses sign sporadically (e.g., through accretion flow reversal), the positive and negative contributions to the variations in α at the orbital frequency would nearly cancel, while the corresponding variations in the flux would not cancel.

With this warning, we first adopt the naive view of F-α correlations in which F and α vary linearly (or at least monotonically), and the sign of α does not switch solely because of flow reversal. In this case, the orbital term in the angular acceleration due to mass accretion is removed by the analysis for orbital parameters. Thus we should also remove the systematic orbital variation in the flux. A simple analysis of the Hakucho data shows that this variation is closely in phase with the anomalistic cycle, with maximum near periapsis. To correct the fluxes in the high energy channel for this orbital variation, we multiply by the factor

$$\Theta(M) = 1 - 0.25 \cos M, \tag{19}$$

where M is the mean anomaly (i.e., measured from periapsis).

We now turn to the question of computing average fluxes corresponding to the average angular accelerations determined in § IVa. In order to minimize dilution of the correlation between F and α, it is necessary that the sampling used to determine the average F on each interval match as closely as possible the sampling used in the determination of the average

α (Appendix C). If we had continuous sampling of the X-ray flux, we would use the second integral $\hat{g}^{(-2)}(t)$ of $\hat{g}(t)$ for the flux sampling function. For the actual data, we have to take the gaps into account.

The power density spectrum of the flux variations (Appendix A) suggests that there is a short time-scale cut-off in the flux variations at a few hours. We there adopt the procedure of counting any flux observation in a satellite orbit (duration about 1.5 hours) as providing full coverage for that orbit, assuming that the variation between consecutive observations is reasonably "smooth." On the other hand, satellite orbits with no observations are treated as missing data. In the same vein, we consolidate all the data within a satellite orbit -- usually covering about one-fourth of the 90 minutes satellite period -- into a single flux average, correcting by the orbital factor $\Theta(M)$ given in equation (19).

The mean flux for the kth interval $[a_k, b_k]$ is then given by the discrete version of equation (C3),

$$F_k = \sum_j \chi(t_{k,j}) h(t_{k,j}) F_{k,j} \Big/ \sum_j \chi(t_{k,j}) h(t_{k,j}) , \qquad (20)$$

where the dummy index j ranges over all satellite orbits within the kth interval, $t_{k,j}$ is the mid-time of the jth orbit, $F_{k,j}$ is the average flux for the jth orbit, h(t) is the second integral of $\hat{g}(t)$, and $\chi(t)$ is a "selector" function defined by

$$\chi(t_{k,j}) = \begin{cases} 1, & \text{for a flux observation in the jth orbit;} \\ 0, & \text{for no flux observation in the jth orbit.} \end{cases} \qquad (21)$$

The uncertainty in the flux estimate due to photon statistics is very much smaller (at least a factor of 100 in variance) than the observed flux variations . In addition to uncertainties from photon statistics, it is likely that other variations in the observed flux which do not reflect actual variations in the luminosity. A primary cause for such flux variations (which was mentioned above) is variable absorbtion along the line of sight. These variations are again relatively small compared to the observed range of variations in the flux, but are difficult to quantify.

In Table 1 we give the uncertainties in the flux estimates F_k based solely on photon statistics.

From the individual estimates of flux from each interval, we compute an over-all mean flux, and the strength of the white noise variations determined from the scatter in the sample $\{F_k\}$ (cf. § III<u>b</u>). The resulting values are reported in Table 2.

<u>c) Results of Correlation Analysis</u>

We computed correlation coefficients of the X-ray flux and angular acceleration at 6-day and 4-day time scales using equation (9). These correlation coefficients ($r^\dagger$) are listed in Table 2, and are uncorrected for dilution.

The uncertainty in the correlation coefficient is as important as the actual value. Also valuable is the distribution function for the statistic used to compute the correlation coefficient, since the test for significance of a non-zero coefficient requires knowing the distribution. Unlike the distribution for r (the statistic for a homogeneous collection of correlation pairs) which depends only on the actual coefficient ρ and the number of correlation pairs, the distribution for $r^\dagger$ cannot be described in a simple fashion and so cannot be readily computed and tabulated. However, the statistic $r^\dagger$ was designed to behave as closely as possible like the statistic r (with an "effective" number of degrees of freedom replacing the actual number of correlation pairs), at least in the limit of near homogeneity for which all correlation pairs have comparable dilution.

In the situation of homogeneous correlation pairs, the variable $z = \tanh^{-1}\rho$ is approximately normal with variance approximately $n - 3$, where n is the number of correlation pairs (see, e.g., Bethea <u>et al</u>. 1984). We adopt this transformation for $\rho^\dagger$, assuming near homogeneity. In this case, n should be replaced by the effective number of degrees of freedom ν, and so the $\pm 1\sigma$ errors for $\rho^\dagger$ are given by

$$\Delta r^\dagger_\pm = \tanh[\tanh^{-1} r^\dagger \pm (\nu - 3)^{-1/2}] - r^\dagger, \qquad (22)$$

with the usual convention of setting $\rho^\dagger = r^\dagger$, as the most likely value for this parameter. These errors are listed in Table 2 along side the estimates for $r^\dagger$.

The undiluted correlation coefficient r' is readily computed from $r^\dagger$ by dividing by the mean dilution $\bar{y}$ (cf. eq. [D6]). Error limits on r' are obtained in a similar fashion. The resulting quantities are also reported in Table 2.

As a check on the accuracy of the error limits derived with the $\tanh^{-1}$ transformation, we also estimated directly the variances of $r^\dagger$ and r' by a scheme involving repeated resampling with replacement from each set of correlation pairs. Resampling schemes such as this are often called "bootstraps"; see, for instance, Efron (1982). An estimate of r' is computed for each resampling, and the variance and standard error of the statistic r' for the entire sample is obtained from the scatter in the resampled estimates. The standard errors for r' obtained in this way are very close to the errors obtained from the distributional properties of the statistic r' (see Table 2).

In addition, we tested whether the hypothesis $\rho = 0$ can be rejected. For this test we again use the diluted statistic $\rho^\dagger$, whose statistical properties closely match those of the standard correlation coefficient. Under the hypothesis $\rho^\dagger = \rho = 0$, the statistic

$$t = r^\dagger \left[\frac{\nu - 2}{1 - r^{\dagger 2}} \right]^{1/2} \tag{23}$$

has Student's t-distribution with $\nu - 2$ degrees of freedom. The two-sided confidence level β is then determined by

$$\beta = \mathrm{Prob}(|t| < |t_{obs}| : \rho^\dagger = 0) , \tag{24}$$

from a table of the t-distribution .

The test for a correlation between flux and α is suggestive, but not compelling; the hypothesis that $\rho = 0$ is unlikely but cannot be rejected

at the 90% level for either the 4- or 6-day averages. However, the F-α correlation plots shown in Figure 3 have a suggestive "butterfly" pattern, with large values for F apparently correlated with both large positive and large negative excursions in α. We are thereby led to investigate F-$|\alpha|$ correlations, at the same 6-day and 4-day time scales. For these computations, we allowed the vertex of the butterfly to be located at a non-zero value of α, which is consistent with physical models. The value $\alpha_f = -2.5 \times 10^{-12}$ rad s^{-2} for the vertex was chosen to maximize the correlation between flux and $|\alpha - \alpha_f|$. We designate this case as "F-$|\alpha|$ correlations."

In line with the discussion at the beginning of § Vb, this case most likely corresponds to the physical situation of flow reversal. In this case the observed orbital variation in the flux does not imply a net orbital variation in the angular acceleration which will bias the orbital parameters, since the orbital term alternates sign, depending on the direction of disc rotation. Thus the orbital flux correction was not applied, since in this case the corresponding variations in the angular acceleration presumably have not been removed in the orbital analysis. In the analysis for F-$|\alpha|$ correlations, the effective degrees of freedom were reduced by 2 to account for the decision to fold the angular acceleration and the determination of the folding parameter α_f. With these minor chages, the F-$|\alpha|$ analysis follows that of the previous F-α analysis. Numerical results are given in Table 2, and the resulting correlation diagrams are shown in Figure 3 along with the earlier results.

The tests on the F-$|\alpha|$ correlations give a slightly more significant result for a non-zero correlation coefficent than do the tests based on F-α correlations. The most significant test is for the hypothesis $\rho = 0$ applied to the F-$|\alpha|$ correlation for the 6-day intervals. This hypothesis is rejected at the 92% level, and this rises to the 96% level for the one-sided test, $\rho \leq 0$. This result has not been significantly weakened by performing a large number of distinct tests, and is very suggestive of a correlation between X-ray flux and rotational acceleration.

VI. DISCUSSION

a) Flow Reversal

The hint of a correlation between X-ray flux and the absolute value of the angular acceleration for Vela X-1 suggests the possibility of flow reversal in the mass-accretion process for this system. We discuss here whether other observational evidence is consistent with flow reversal in this system, but a full treatment of the theoretical implications will be left for later papers (e.g., Lamb et al. 1988).

For simplicity, we assume that the relationship between instaneous F and α is monotonic and close to linear for "normal" accretion flow (in the same direction as the neutron star rotation), and that essentially the same relationship holds between F and $-\alpha$ for flow in the reverse direction. The form of the observed F-α relationship then depends largely on whether the reversal timescale is longer or shorter than the averaging timescale for α and F. If the reversal timescale is longer, then the F-α diagram will display two distinct lines corresponding to the two cases of direct and reverse accretion flow. However, if the reversal time scale is shorter, then the diagram will "fill in" (Lamb 1985) since each observed value for α will be an average over one or more reversals in the flow direction. The appearce of the F-α diagram for the analysis of Vela X-1 presented here suggests that the reversal time scale is longer than the averaging time scale of 6 days. This is only a guess, and we do not have enough data (11 correlation pairs) to make a definite test for the size of the reveral timescale.

Flow reversal will also have an affect on the power density spectrum of the fluctuations in the angular acceleration. We interpret the variations of the X-ray flux -- almost 100% modulated on the timescale of several hours (see Appendix A) -- as evidence for noise in the mass accretion process. Flow reversal causes an alternation in the direction of the angular acceleration of the pulsar, thereby introducing variations in the angular acceleration about as large as the variations from the noisy accretion process. The timescale for flow reversal appears to be an order of magnitude larger than the timescale for variations in mass accretion,

corresponding to a frequency bandwidth one-tenth as large. Although the power in the two noise components is comparable, the power density for the reversal fluctuations is ten times the power density for the variations in mass accretion, with an increase in power density at analysis frequencies shorter than $f \approx (2\pi \cdot 6 \text{ days})^{-1}$. The absence of a large jump in the power density spectrum of the variations in α is therefore evidence against flow reversal in Vela X-1. Unfortunately, we have no additional evidence at this time which will aid in reconciling these conflicting conclusions about flow reversal in Vela X-1.

b) Guidelines for Future Studies

Although the present investigation has not produced a decisive result regarding F-α correlations in Vela X-1, we can still use the experience gained to help establish guidelines for future F-α studies.

Studies of the noise properties of both flux and angular acceleration should be made before an F-α correlation analysis is undertaken for a particular data set. Both variables should show significant variations whose statistical properties indicate that they could arise from the same basic process. In particular, the power spectra for F and α should be have similar behavior at sufficiently low frequencies, where variations in angular acceleration from mass accretion dominate variations induced from pulse shape noise . In the following general discussion, we assume that the power density spectrum of variations in α from mass accretion is flat (power-law with exponent equal to zero), while the spectrum of variations from pulse-shape noise obeys a power law with exponent equal to four.

An important concept in evaluating whether an F-α correlation analysis is appropriate for a particular data set is the "crossover timescale" T_{CO}, taken to be the time interval on which the rms variations in the angular acceleration from flucuations in mass accretion equal the rms variations induced by pulse-shape noise. We will define T_{CO} as the time interval on which an estimate of angular acceleration has equal variances from the two noise processes as given by equations (C4a) and (C11) in Appendix C. In general, both variances scale with the interval length T: $\tau_\alpha^2 = S_\alpha K_\alpha / T^5$ (mass accretion fluctuations) and $\sigma_\alpha^2 = S_\phi K_\phi / T$

(pulse-shape noise) where K_α and K_ϕ are constants whose values depend on the specific method of computing the angular acceleration. For an estimate of the angular acceleration obtained from the quadratic coefficient of a second degree polynomial fit to pulse phase, the timescale T_{co} at which $\tau_\alpha^2 = \sigma_\alpha^2$ is given by

$$T_{co} = (504)^{1/4} (S_\phi / S_\alpha)^{1/4} \approx 4.74 (S_\phi / S_\alpha)^{1/4} . \qquad (25)$$

This expression is closely related to equation (12) of Boynton et al. (1986), which gives the "crossover frequency" at which the power densities of the two noise processes are equal, $1/f_{co} = 2\pi (S_\phi / S_\alpha)^{1/4}$. The small difference in the numerical coefficients in the expressions for T_{co} and $1/f_{co}$ reflects the distinction between the two estimates; f_{co} arises from a comparision of power densities at a precise frequency, while T_{co} comes from comparing power within a broad frequency band with $1/T_{co}$ representing a typical frequency in that band.

As indicated in § IIIa, the crossover timescale T_{co} sets a definite lower bound on the range of timescales appropriate for the study of F-α correlations. Moreover, the maximum feasible timescale is generally not much larger, since the number of independent correlation pairs diminishes as the analysis interval is increased. A compromise must be struck between either a large number of correlation pairs with a corresponding reduction in the expected correlation coefficient, or a small number of pairs with very little reduction. This tradeoff can be expressed in terms of the likelihood of detecting a correlation between F and α, when the correlation has a specified nonzero value ρ. This likelihood should be as large as possible, over the range of possible subdivisions of a given data set with total observing time T_{tot}. This maximization problem is facilitated by applying the transformation $z = \tanh^{-1} r$ to the correlation coefficient r; z is approximately normal with variance $(n-3)^{-1}$ (Bethea et al. 1985). We then maximize the ratio $z/(\mathrm{var}\, z)^{1/2}$, as the size of the analysis interval is varied.

In implementing this maximization procedure, it is necessary to specify the true correlation coefficient ρ between F and α, as well as the

total data span T_{tot}. If the length of the analysis interval is denoted by T, then the number of independent correlation pairs is $n = T_{tot}/T$ and the observed correlation coefficient is $\rho/[1+(T_{co}/T)^4]^{1/2}$, including the dilution due to pulse shape noise in α (cf. eq. [C12]). With these subsitutions in the ratio $z/(\mathrm{var}\, z)^{1/2}$, we obtain the expression

$$\left(\frac{T_{tot}}{T} - 3\right)^{1/2} \tanh^{-1} \frac{\rho}{[1+(T_{co}/T)^4]^{1/2}}, \qquad (26)$$

which we maximize with respect to T. Unfortunately, the analytic maximization of equation (26) does not result in a simple expression in terms of the various parameters. However, in the limits of a small correlation coefficient ($|\rho|$ less than 0.5) and a large number of correlation pairs (n larger than 25 or so), an approximate solution can be obtained by replacing $\tanh^{-1} z$ by z and substituting n for $n - 3$ in var z. The resulting optimum timescale is $T \approx 3^{1/4} T_{co} \approx 1.3 T_{co}$, to lowest order independent of both ρ and T_{tot}. Calculation shows that the optimum length is shorter for small sample sizes (less than 25 or so), and longer for large $|\rho|$. In any event the minimum is fairly broad, and any value of T between T_{co} and $2T_{co}$ will be close to optimum unless the sample size is very small or $|\rho|$ is close to 1.

This argument establishes the optimum length for the analysis interval, irrespective of whether a detection of an actual correlation is likely to be established. The minimum number of correlation pairs needed to establish a nonzero correlation clearly depends on the actual value of the correlation coefficent. To get a 2σ detection, we need to have $z/(\mathrm{var}\, z)^{1/2} = 2$. Using the guideline that the analysis interval should be approximately $1.3T_{co}$ and interpreting T_{tot}/T as n, we can set the expression in equation (26) equal to 2 and solve for n, Thus, if $\rho = 0.5$, a minimum of 22 correlation pairs is required to assure a reasonable likelihood of a 2σ detection, with more or less pairs for smaller or larger ρ, respectively.

The minimum data span required is approximately $1.3nT_{co}$. It is therefore essential to choose a source with a short crossover timescale, preferably a few hours, in order to keep the total data span

to a practical length. A small T_{CO} is dependent on a large S_α (noise from the mass-accretion process) or a small S_ϕ (noise from pulse-shape variations).

Both conditions are more likely to be satisfied by a rapidly-spinning pulsar than by a slowly-spinning one. First, a rapidly-spinning pulsar is likely to be a "fast" pulsar in the sense of Ghosh and Lamb (1979b), and hence is likely to have large torques and relatively large torque noise from the mass accretion process. Second, in considering contributions to S_ϕ, Boynton et al. (1986) have argued that the dominant pulse shape variations for high-count rate data is likely to be fluctuations intrinsic to the source as opposed to variations due to counting statistics. We have found that the size of pulse-to-pulse fluctuations in Her X-1 and Vela X-1 are nearly the same, even though the properties of these pulsar are quite different and their pulse frequencies differ by a factor of 250. If this property is found to hold for all pulsars, then the noise strength S_ϕ due to intrinsic pulse shape fluctuations would be inversely proportional to the number of pulses per unit time (i.e., the pulse frequency), and so should be smallest for the most rapidly-spinning pulsars. Thus the relatively rapid pulsars Her X-1, Cen X-3 and LMC X-1 are more promising candidates for future study than the much slower Vela X-1.

VII. CONCLUSIONS

We have analyzed the usable Hakucho data on Vela X-1 for correlations between X-ray flux and angular acceleration in the rotation of the neutron star. Our most significant result is a detection of a correlation between the flux and $|\alpha|$, significant at the 96% level. This result suggests the possibility of flow reversal in mass accretion for Vela X-1. We do not have any other definite, supporting evidence of this possibility, but the possibily of flow reversal in Vela X-1 should encourage F-α studies of other X-ray pulsars which might also be fed by wind accretion.

A major emphasis of this study has been the development of methods to handle peculiarities in the Vela X-1 data which complicated a direct application of standard correlation analysis. The major difficulties

inherent in our data were a sampling mismatch between X-ray flux and pulsar angular acceleration; the dilution in correlation resulting from the mismatch; and the treatment of correlation pairs with different dilutions due to inhomogeneties in the data. The solutions to these difficulties are discussed with a fair amount of detail to allow use in future studies.

The primary application of the methods developed here is to pulsars for which the angular acceleration can be determined only at time scales longer than the time scale for variations in the X-ray flux and angular acceleration. In some sources this may not be true -- for instance, in the transient source EXO 2030+375 (Parmar et al. 1988) -- and the statistical treatment presented here will not be necessary. (However, transient sources present other problems, such as ambiguities in separating accelerations in the pulse frequency due to orbital motion from accelerations in the rotation rate of the neutron star, particularly if the flare lasts for less than one binary orbit.)

Finally, the methods discussed here are useful in planning future F-α studies, such as the amount of data needed to obtain an adequate number of correlation pairs and underlining the necessity for obtaining data with nearly continuous sampling of the X-ray flux to avoid a sampling mismatch with the angular acceleration.

We thank Prof. Fred Lamb for helping to bring together his Japanese and U. S. colleagues in this collaborative effort, and for his constant encouragement in this research. We are also grateful to T. Ohashi, N. Kawai, and the other members of the Hakucho team for preparation of the Hakucho data sets for the analysis presented here. We also thank J. Zeh and M. Newton of the Department of Statistics at the University of Washington for helpful suggestions regarding statistical procedures. Two of us, P. B. and J. D., want to express our appreciation to our Japanese hosts for their hospitality during several visits and to the Japanese Society for the Promotion of Science and the Yamada Science Foundation for their generous support. This work was also funded by NASA grants NAGW-805 and NAGW-1133 (at the University of Washington).

APPENDIX A.
POWER DENSITY SPECTRUM OF THE X-RAY FLUX FROM VELA X-1

The fluxes used in the power-spectral analysis were from the Hakucho high-energy channel (9--22 keV), normalized to center collimator. The high-energy channel was chosen over the low-energy channel (2--9 keV) because it was less affected by variable cold-matter absorbtion due to material in the vicinity of the source. The fluxes were given in counts per second, averaged over one pulsation period. These points were further consolidated to one point per satellite orbit, and data taken during eclipse were ignored.

The power spectrum of these fluxes was computed using a variant of the simple periodogram:

$$a_f = \sum_{k=1}^{n} \Delta F_k \cos 2\pi f t_k \Big/ \sum_{k=1}^{n} \cos^2 2\pi f t_k \,, \tag{A1a}$$

$$b_f = \sum_{k=1}^{n} \Delta F_k \sin 2\pi f t_k \Big/ \sum_{k=1}^{n} \sin^2 2\pi f t_k \,, \tag{A1b}$$

where the sums range over all data points in a particular interval. However, to avoid domination of the rest of the power spectrum by the relatively large constant term, we replace each F_k by its residual from the mean within the interval,

$$\Delta F_k = F_k - \bar{F} \,, \tag{A2}$$

$$\bar{F} = \frac{1}{n} \sum_{k=1}^{n} F_k \,. \tag{A3}$$

Likewise, we replace $\cos 2\pi f t_k$ and $\sin 2\pi f t_k$ by the residuals from each of their respective means, obtaining modified versions of equations (A1a) and (A1b),

$$a_f = \sum_{k=1}^{n} \Delta F_k \Delta \cos 2\pi f t_k \Big/ \sum_{k=1}^{n} \Delta \cos^2 2\pi f t_k \,, \tag{A4a}$$

$$b_f = \sum_{k=1}^{n} \Delta F_k \Delta \sin 2\pi f t_k / \sum_{k=1}^{n} \Delta \sin^2 2\pi f t_k \, . \qquad (A4\underline{b})$$

To convert the periodogram to a power density spectrum, we normalize by multiplying by the time covered by the observations, excluding essential gaps in the data record. In computing this time coverage, we also take into account that the flux variations are suppressed at time scales shorter than the minimum spacing of the data points Δt_{sat} = 0.067 days, the sidereal period of the Hakucho orbit). Thus the total "live" time is given by $\Delta T = n\Delta t_{sat}$, and the power spectrum is

$$P_f = n\Delta t(a_f^2 + b_f^2) \, . \qquad (A5)$$

The single periodogram determined from the entire span of data does not give an accurate representation of the power density spectrum at all analysis frequencies, since sampling periodicies transfer power between remote frequencies. In order to circumvent this difficulty, we divided the the data into subsets on a range of timescales with subset divisions chosen to provide reasonably uniform data spacing within each subset. The time scales chosen as nominal lengths for subsets were: 1000, 83, 20, 10, 5, 0.5 and 0.25 days. Power estimates were computed at each of these periods, and for shorter periods in some cases ~~(see Table II)~~. There are two gaps in this hierarchy of time scales -- around 360 days due to annual sampling of the source, and around 1 day due to daily sampling.

All the power estimates at the same period were averaged, thus producing pooled estimated at 11 time scales. In addition, the noise contribution from photon statistics to these power estimates were computed from the corresponding errors, σ_k, on the individual flux estimates:

$$\mathrm{var}(a_f) = \sum_{k=1}^{n} \sigma_k^2 \cos 2\pi f t_k / \Big[\sum_{k=1}^{n} \cos^2 2\pi f t_k \Big]^2 , \qquad (A6\underline{a})$$

$$\mathrm{var}(b_f) = \sum_{k=1}^{n} \sigma_k^2 \sin 2\pi f t_k \Big/ \Big[\sum_{k=1}^{n} \sin^2 2\pi f t_k \Big]^2 , \qquad \text{(A6b)}$$

$$P_{f,\mathrm{phot}} = n\Delta t [\mathrm{var}(a_f) + \mathrm{var}(b_f)] . \qquad \text{(A6c)}$$

The resulting power spectrum is shown in the accompanying Figure 1.

In every case, the observed power density is much larger than that from photon noise. In addition, there is a deficiency in power density at the shortest periods, $1/f \approx 0.5$, 0.25 days. This result confirms what is fairly evident in the light curves themselves -- that the flux varies substantially (50% or more modulation) on the time scale of a couple of hours or longer, but the variations are much smoother on shorter time scales. [A formal fit with a Gaussian roll off gives a smoothing time scale of about 0.05 days.] There is no evidence in the power spectrum for variations around 5--10 days (around the orbital period), but this is understandable because a narrow feature is greatly diluted in a broad-band version of the power spectrum.

APPENDIX B.
SAMPLING OF ANGULAR ACCELERATION

An important consideration in testing for a correlation between flux and angular acceleration is selecting a method for estimating the angular acceleration from a given segment of data, and understanding how this estimate effectively averages the instaneous acceleration. A seemingly straightforward estimate is suggested by the low-order terms of a Taylor's expansion,

$$\phi(t) = \phi_o + \Omega_o (t - t_o) + \frac{\alpha_o}{2}(t - t_o)^2 . \qquad \text{(B1)}$$

This expression indicates that the quadratic coefficent in a least-squares polynominal fit to the the phase is a reasonable estimate for the angular acceleration. Mechanically following this prescription is not enough for our purposes. We need to understand how the estimate of angular acceleration arises as an average of the instantaneous acceleration over the interval, in order to average the X-ray flux in a similar fashion. Furthermore, we want to insure that the estimate is efficient in the statistical sense; that is, that the variance contribution from pulse-shape noise (white noise in pulse phase) for this estimate of the angular acceleration is small compared to the pulse-shape variance incurred in alternative methods.

A natural setting for discussing both of these points is an existing framework for estimating red noise in rotation (Deeter and Boynton 1982; Deeter 1984), and for propagating red noise into parameter estimates (Appendix to Boynton et al. 1986). In the latter reference, several points of interest to the present discussion are examined. First, when data $x(t)$ in an interval $[a, b]$ are fit by a set of functions $g_j(t)$ with coefficients β_j,

$$x(t) = \sum_j \beta_j g_j(t) + \epsilon(t) . \qquad \text{(B2)}$$

the solution which minimizes the sum squared residuals can be expressed as a vector of linear functionals applied to the data,

$$\beta_j = \int_a^b \hat{g}_j(t)x(t)\,dt\,. \tag{B3}$$

Second, the functions $\hat{g}_j(t)$ are "dual" to the fitted functions in the sense that the two sets of functions are cross-orthogonal,

$$\int_a^b g_j(t)\hat{g}_k(t)\,dt = \delta_{jk}. \tag{B4}$$

Furthermore, if the first m functions are monomials in t up to degree $m-1$, then as a special case of equation (B4) the remaining dual functions are orthogonal to the low-degree monomonials,

$$\int_a^b \hat{g}_j(t)t^k\,dt = 0, \qquad \text{for } j \geq m+1,\ k \leq m-1. \tag{B5}$$

Applying this result to the present situation, we consider fitting pulse phase data by a constant term, a linear term, and any third funtion g(t),

$$\phi(t) = \phi_o + \Omega_o(t - t_o) + \beta g(t)\,. \tag{B6}$$

Then the parameter β is obtained from the data by using the dual function $\hat{g}(t)$ as a sampling function,

$$\beta = \int_a^b \hat{g}(t)\phi(t)\,dt. \tag{B7}$$

Furthermore, $\hat{g}(t)$ is orthogonal to two lowest-degree monomials,

$$\int_a^b g(t)t^k\,dt = 0. \qquad \text{for } k = 0,1. \tag{B8}$$

But, as discussed by Deeter and Boynton (1982), this is exactly the condition needed to rewrite equation (B7) via integration by parts to show

explicity how angular acceleration [the second derivative of $\phi(t)$] is sampled,

$$\beta = (-1)^2 \int_a^b \hat{g}^{(-2)}(t)\alpha(t)\, dt. \tag{B9}$$

The integrated terms drop out provided we choose the particular second integral which vanishes at the end points of the interval,

$$\hat{g}^{(-2)}(a) = \hat{g}^{(-2)}(b) = 0\,. \tag{B10}$$

We can now return to the original topic: how does the quadratic term in equation (B1) sample the angular acceleration in the interval [a, b]? As an illustration, we take $g(t) = (1/2)(t - t_o)^2$ where $t_o = (a+b)/2$, with continuous sampling of pulse phase in the interval. Then, by direct calculation we have

$$\hat{g}(t) = \frac{15}{4\Delta t^5}\left[3(t - t_o)^2 - \Delta t^2\right], \tag{B11}$$

and

$$\hat{g}^{(-2)}(t) = \frac{15}{16\Delta t^5}\left[\Delta t^2 - (t - t_o)^2\right]^2, \tag{B12}$$

where $\Delta t = (b - a)/2$ is the half-length of the interval. Note that $\hat{g}^{(-2)}(t)$ is a bell-shaped function within the interval [a, b], which vanishes only at the endpoints. Using the coefficient of the quadratic term as an estimator of the angular acceleration is therefore an intuitively appealing weighted average of the instantaneous values of the acceleration over the interval.

Furthermore, these basic virtues of $\hat{g}^{(-2)}(t)$ carry over to cases of non-continuous sampling, as long as the sampling is approximately uniform. Even in the extreme case where the quadratic function is fit to a discrete set of points in the interval, the function $\hat{g}^{(-2)}(t)$ will still be continuous, consisting of linear segments. The crucial implication of this result is that the instaneous angular acceleration at every point within the interval contributes to estimate of the average acceleration, even for discontinous sampling.

APPENDIX C.

SAMPLING MISMATCH BETWEEN X-RAY FLUX AND ANGULAR ACCELERATION

One major difficulty in the correlation analysis is obtaing averages for F and α which are strictly concurrent. A suitable average of the angular acceleration is the quadratic coefficient in a polynomial fit to pulse phase, and is effectively a weighted average of the instaneous $\alpha(t)$ over the entire interval even though discontinously sampled (Appendix B). The instaneous F(t), on the other hand, may be used to compute an average flux that is valid only on the subinterval containing usable observations.

We first consider the effect on the observed correlation from this mismatch in sampling, laying aside the consideration of effect of other sources of noise in either the flux or the angular acceleration. We consider the case where data is available only on a chopped-up subset of a specified interval [a, b]. This subset can be identified through a chacteristic function,

$$\chi(t) = \begin{cases} 1, & \text{where the flux is observed;} \\ 0, & \text{elsewhere.} \end{cases} \tag{C1}$$

The angular acceleration α is estimated by a quadratic function fit to the phases. As explained in Appendix B, this is tantamount to sampling $\alpha(t)$ continuously with a bell-shaped function h(t),

$$\alpha = \int_a^b h(t)\alpha(t)\, dt\,. \tag{C2}$$

[h(t) is an appropriate second integral of a function $\hat{g}(t)$ which samples pulse phase discontinously.] For the purposes of computing and interpreting a correlation coefficient, it is necessary to match the sampling of F as closely as possible to that for α. Thus the same sampling function h(t) should be used for F(t), but by necessity it will be restricted to the subset of observations,

$$F = \int_a^b h(t)\chi(t)F(t)\, dt \Big/ \int_a^b h(t)\chi(t)\, dt\,. \tag{C3}$$

The variances of these estimates for α and F can be computed from the sampling functions and the noise strengths,

$$\tau_\alpha^2 = S_\alpha \int_a^b [h(t)]^2 \, dt , \tag{C4a}$$

$$\tau_F^2 = S_F \int_a^b [h(t)\chi(t)]^2 \, dt \Big/ \Big[\int_a^b h(t)\chi(t) \, dt\Big]^2 . \tag{C4b}$$

According to equations (1a,b) in the text, the factors following S_α and S_F can each be identified with an inverse time scale,

$$T = \Big[\int_a^b \{h(t)\}^2 \, dt\Big]^{-1} , \tag{C5a}$$

$$T' = \Big[\int_a^b h(t)\chi(t) \, dt\Big]^2 \Big/ \int_a^b [h(t)\chi(t)]^2 \, dt . \tag{C5b}$$

In general, $T' < T < (b - a)$. These inequalities are intuitively sensible -- in particular, α is sampled with a bell-shaped function whose mean width is less than the length of the interval $[a, b]$, and the sampling of F is over an even shorter interval.

The covariance between F and α is affected only by data within the subset of observations where they are both sampled. The easiest way to compute this covariance is to introduce averages α' and α'' on and off the subset of observations,

$$\alpha' = \int_a^b h(t)\chi(t)\alpha(t) \, dt \Big/ \int_a^b h(t)\chi(t) \, dt , \tag{C6a}$$

$$\alpha'' = \int_a^b h(t)[1 - \chi(t)]\alpha(t) \, dt \Big/ \int_a^b h(t)[1 - \chi(t)] \, dt . \tag{C6b}$$

Then $\alpha = x\alpha' + (1 - x)\alpha''$, where x is the weighted fraction of time under observation,

$$x = \int_a^b h(t)\chi(t) \, dt \Big/ \int_a^b h(t) \, dt . \tag{C7}$$

The variance for α' has the same scaling factor as that for F, $\mathrm{var}\,\alpha' = S_\alpha/T'$. The covariance between F and α is then given by

$$\mathrm{cov}(F, \alpha) = \mathrm{cov}(F, x\alpha') = x\rho\frac{(S_F S_\alpha)^{1/2}}{T'}, \tag{C8}$$

where ρ is the correlation coefficient for concurrently sampled F and α (cf. eq. [2] in the text). The diluted correlation coefficient between the mismatched averages is

$$\rho^* = \frac{\mathrm{cov}(F, \alpha)}{\tau_F \tau_\alpha} = x(T/T')^{1/2}\rho\,. \tag{C9}$$

As an approximation, $T'/T \approx x$ (with equality when the data dropout is uniformly distributed on the interval), giving $x(T/T')^{1/2} \approx x^{1/2}$ as an approximation for the dilution factor.

We now add the complication of variations in F and α beyond those due to fluctuations in the mass accretion rate,

$$\mathrm{var}\,F = \tau_F^2 + \sigma_F^2, \tag{C10a}$$

$$\mathrm{var}\,\alpha = \tau_\alpha^2 + \sigma_\alpha^2\,. \tag{C10b}$$

Excess variations in the X-ray flux include noise due to finite count rate and unmodeled variations in detector area. These variations are likely to conform closely to white noise; for our data they are small and are ignored. On the other hand, the excess variations in α arising from fluctuations in pulse shape (including noise due to finite count rate) have a completely different character. These fluctuations are observed to be white in pulse phase (Deeter et al. 1987), and so can be characterized by a noise strength S_ϕ which is distinct from S_α. Indeed, the noise propagation law is different (cf. eq. [C4a])

$$\sigma_\alpha^2 = S_\phi \int_a^b [\hat{g}(t)]^2\,dt\,. \tag{C11}$$

This, in fact, is the variance that arises in the least-squares determination of α in the quadratic fit to pulse phase.

The overall dilution, including the effect of excess noise, is given by an expression similar to equation (C9) with τ_F^2 and τ_α^2 replaced by the total variances,

$$\rho^* = \frac{\mathrm{cov}(F, \alpha)}{(\mathrm{var}\, F\, \mathrm{var}\, \alpha)^{1/2}} = x \left[\frac{T}{T'}\right]^{1/2} \left[\frac{\tau_F^2}{\tau_F^2+\sigma_F^2}\right]^{1/2} \left[\frac{\tau_\alpha^2}{\tau_\alpha^2+\sigma_\alpha^2}\right]^{1/2} \rho = y\rho\,. \qquad (C12)$$

In the case of homogeneous data, where both effects are the same for all samples included in the correlation analysis, the dilution factor is also the same for all samples. In this case, ordinary correlation analysis is applicable. However, our samples are sufficiently inhomogeneous to require a modification to incorporate weights into the formula for the correlation coefficent, as discussed in detail in Appendix D.

APPENDIX D.
COMBINING INDEPENDENT CORRELATION PAIRS

As discussed in the text, it may be possible to characterize correlated variations in X-ray flux and angular acceleration (arising from the mass-accretion process) by a correlation coefficient ρ and two noise strengths, S_F and S_α. In this Appendix, we discuss modifications in a standard method for estimating ρ to accomodate data with less than ideal properties.

For homogeneous data consisting of correlation pairs (F_k, α_k) with identical statistical properties the natural statistic for investigating the correlation cofficient is

$$r = \frac{(1/n)\sum_k (F_k - \bar{F})(\alpha_k - \bar{\alpha})}{\tau_F \tau_\alpha}, \qquad (D1)$$

where the index k ranges over the correlations pairs, and τ_α and τ_F are the observed rms scatter in the two variables (see, for instance, Green and Margerison [1978]). The expectation of this statistic is the true correlation coefficent, $E(r) = \rho$ (ignoring a bias of order $1/n$ which is less than the uncertainty in r). As explained in the text, we have to modify equation (D1) to accomodate several complications in our data. These complications include:

(1) The correlated component is expected to have the character of white noise, and the variance of this component therefore scales inversely with the length of the averaging interval (eqs. [1a,b] in the text). Due to sampling irregularities, the interval lengths in our sample are not identical, and so the individual variances are not uniform among the correlation pairs.

(2) The observed correlation coefficient is diluted because of the mismatch in sampling between F and α (Appendix C), and the dilution is different for the various pairs (F, α).

(3) There are excess variations in both F and α besides the fluctuations due to mass accretion, which cause a further dilution in

the observed correlation coefficient beyond that due to the mismatch in sampling. Particular care must be taken in accounting for the excess variations in the angular acceleration, since they have a distinctly different character from the intrinsic variations.

Points (1) and (3) specify individual variances for each correlation pair, in contrast to the uniform variances τ_F^2 and τ_α^2 indicated in the denominator of the right-hand side of equation (D1), and in addition point (3) specifies that the individual variances include a contribution from excess noise. We therefore introduce the total variances $\tau'_{F,k}$ and $\tau'_{\alpha,k}$, defined as

$$\tau'^2_{F,k} = \tau^2_{F,k} + \sigma^2_{F,k}\,, \tag{D2a}$$

$$\tau'^2_{\alpha,k} = \tau^2_{\alpha,k} + \sigma^2_{\alpha,k}\,, \tag{D2b}$$

where $\tau^2_{F,k}$ and $\tau^2_{\alpha,k}$ represent the intrinsic noise due to mass accretion for the kth subset of the data, and the corresponding σ^2's the variance due to excess noise. The first modification to equation (D1) is to replace division by $\tau_F\tau_\alpha$ outside the summation with division by $\tau'_{F,k}\tau'_{\alpha,k}$ <u>inside</u> the summation.

The first modification would suffice if all correlation pairs had a common correlation coefficent even if they had different variances. However, because of non-uniform dilution (points [2] and [3]) the observed correlation coefficent will differ among the pairs. To accomodate this complication, we further modify equation (D1) to produce a weighted estimate of the correlation coefficient,

$$r' = \sum_k w_k \frac{(\alpha_k - \bar{\alpha})\,(F_k - \bar{F})}{y_k \tau'_{\alpha,k}\tau'_{F,k}} \Big/ \sum_k w_k\,, \tag{D3}$$

where the divisors y_k correct for dilution in the various estimates, and the weights are to be determined by a minimum variance principal applied to r'. We therefore investigate the variances of the individual summands in

equation (D3),

$$r'_k = \frac{(\alpha_k - \bar{\alpha})(F_k - \bar{F})}{y_k \tau'_{\alpha,k} \tau'_{F,k}}, \tag{D4}$$

For the purpose of deriving relative weights for the various r'_k we assume that the denominators $y_k \tau'_{F,k} \tau'_{\alpha,k}$ are known exactly; in this case, $E(r'_k) = \rho$ and

$$\text{var } r'_k = [1 - (y_k \rho)^2]/y_k^2 \approx 1/y_k^2 . \tag{D5}$$

The approximation in equation (D5) is valid provided the <u>diluted</u> correlation $y_k \rho$ is close to zero. The statistic r' with minimum variance is then specified by weighting the terms according to their inverse variances, $w_k = y_k^2$, thereby obtaining

$$r' = \sum_k y_k \frac{(\alpha_k - \bar{\alpha})(F_k - \bar{F})}{\tau'_{\alpha,k} \tau'_{F,k}} \Big/ \sum_k y_k^2 . \tag{D6}$$

The expectation of this statistic is ρ and its variance is $1/\sum_k y_k^2$, at least in the limit of all quantities $y_k \rho$ close to zero.

There is a minor problem with the statistic r' which prevents it from being used directly as an approximation in statistical tests usually applied to r. This problem is illustrated by considering the limiting case of identical dilution y for all terms, whereby the statistic r' reduces to r/y. The factor y is extraneous in the application of the usual statistical tests, which are based on the <u>observed</u> (i.e., diluted) statistic r. To alliviate this difficulty, we introduce the statistic $r^\dagger$ with a slightly different normalization,

$$r^\dagger = \sum_k y_k \frac{(\alpha_k - \bar{\alpha})(F_k - \bar{F})}{\tau'_{\alpha,k} \tau'_{F,k}} \Big/ \sum_k y_k . \tag{D7}$$

The expectation of $r^\dagger$ is given by

$$E(r^\dagger) = \rho \sum_k y_k^2 \Big/ \sum_k y_k = \bar{y}\rho , \tag{D8}$$

wherein the factor $\bar{y} = \sum_k y_k^2 / \sum_k y_k$ can be regarded as the mean dilution for the statistic $r^\dagger$. Likewise, the variance is given by

$$\text{var}\, r^\dagger = \sum_k y_k^2 \Big/ \Big[\sum_k y_k\Big]^2, \tag{D9}$$

in the limit that $\bar{y}\rho$ is close to zero. As with the statistic r, this variance is related inversely to the number of terms in the summation. For $r^\dagger$, however, only those tems with the least dilution carry full weight is the summation and the effective number of summands given by the inverse variance, $\nu = 1/\text{var}\, r^\dagger$, is less than the actual number of correlation pairs, n. There is clearly better justification to use ν rather than n for the number of correlation pairs when approximating the distribution for $r^\dagger$ by a distribution for r.

TABLE 1
Flux and Angular Acceleration Data Used in Correlation Analysis

t_{mid} (JD− 2,440,000)	T_α (days)	α (p rad s^{-2})	T_F (days)	x (flux coverage)	F_x [a] (cnt s^{-1} cm^{-2})	F_x [b] (cnt s^{-1} cm^{-2})
		6-day Intervals				
4310.63 . . .	4.32	−1.9 ± 0.4	1.28	0.325	0.100±0.001	0.113±0.001
4319.23 . . .	4.47	−1.5 0.4	1.12	0.257	0.075 0.001	0.074 0.001
4596.86 . . .	4.30	+0.7 1.0	0.56	0.135	0.107 0.002	0.112 0.002
4615.61 . . .	4.90	−4.4 0.4	1.59	0.313	0.122 0.001	0.138 0.001
4625.35 . . .	3.15	−4.9 0.9	0.95	0.329	0.084 0.001	0.101 0.002
4668.80 . . .	3.84	−2.5 0.5	0.92	0.231	0.134 0.002	0.144 0.002
4991.96 . . .	4.41	+3.4 1.3	0.87	0.212	0.186 0.002	0.221 0.002
5000.39 . . .	3.78	+2.8 1.2	0.90	0.249	0.166 0.002	0.163 0.002
5009.36 . . .	3.75	−0.4 1.3	1.11	0.320	0.066 0.002	0.069 0.002
5028.50 . . .	3.80	−2.3 1.3	2.14	0.569	0.078 0.002	0.089 0.002
5323.67 . . .	3.74	−2.4 ± 2.0	0.25	0.076	0.066±0.004	0.071±0.004
		4-day Intervals				
4309.98 . . .	3.03	+1.6 ± 1.2	0.81	0.300	0.108±0.002	0.119±0.002
4311.61 . . .	3.13	−5.9 1.2	1.15	0.374	0.094 0.001	0.112 0.001
4318.02 . . .	2.49	+0.5 1.7	0.83	0.358	0.081 0.002	0.070 0.001
4320.62 . . .	3.27	−0.5 1.7	0.59	0.178	0.082 0.002	0.097 0.002
4597.56 . . .	3.11	−0.3 1.5	0.40	0.140	0.098 0.003	0.114 0.003
4614.35 . . .	3.04	−2.4 1.0	0.74	0.275	0.113 0.002	0.104 0.002
4616.67 . . .	3.28	−4.9 0.7	1.05	0.362	0.135 0.002	0.165 0.002
4625.35 . . .	3.15	−4.9 0.9	0.95	0.329	0.084 0.001	0.101 0.002
4633.72 . . .	2.41	+1.5 2.6	0.79	0.370	0.116 0.002	0.139 0.002
4668.10 . . .	3.07	−2.0 1.1	0.76	0.239	0.129 0.002	0.125 0.002
4676.61 . . .	2.38	−1.8 1.3	0.53	0.218	0.056 0.002	0.048 0.002
4955.13 . . .	3.12	+0.8 2.1	0.90	0.313	0.145 0.002	0.150 0.002
4992.61 . . .	3.05	+5.4 2.3	0.64	0.228	0.224 0.002	0.275 0.002
5000.43 . . .	3.73	+2.5 1.3	0.88	0.248	0.165 0.002	0.163 0.002
5027.78 . . .	2.88	−0.1 2.8	1.71	0.618	0.088 0.003	0.097 0.003
5029.24 . . .	2.64	−4.3 3.0	1.34	0.517	0.063 0.003	0.077 0.003
5323.67 . . .	3.74	−2.4 ± 2.0	0.25	0.076	0.066±0.004	0.071±0.004

[a] X-ray flux without orbital correction.

[b] X-ray flux corrected by multiplying by the factor $1 - 0.25 \cos M$, where M is the orbital mean anomaly of Vela X-1.

TABLE 2
Correlations between Flux and Acceleration

Quantity	F-α Correlations		F-$\lvert\alpha\rvert$ Correlations	
	6-day Intervals	4-day Intervals	6-day Intervals	4-day Intervals
$\bar{F}$ (cnt cm^{-2} s^{-1})	0.116	0.119	0.106	0.118
S_F (cnt cm^{-4} s-1) ...	170	162	133	114
$\bar{\alpha}$ (p rad s^{-2})	-1.31	-1.25	1.94	2.45
S_α (10^{-18} rad^{-2} s^{-3}) .	1.86	1.76	0.72	0.26
Number of (F,α) pairs .	11	17	11	17
ν (effective dof)	10.4	16.3	8.2[e]	13.4[e]
$r^\dagger$	$0.40^{+0.26}_{-0.34}$	$0.34^{+0.22}_{-0.26}$	$0.59^{+0.22}_{-0.36}$	$0.39^{+0.23}_{-0.29}$
$\bar{y}$[a]	0.509	0.485	0.469	0.333
r' $(= r^\dagger/\bar{y})$	$0.78^{+0.51}_{-0.68}$	$0.71^{+0.45}_{-0.54}$	$1.26^{+0.47}_{-0.77}$	$1.17^{+0.69}_{-0.87}$
$\sigma_{r'}$[b]	±0.86	±0.72	±0.63	±0.77
t[c]	1.26	1.37	2.09	1.55
β[d]	0.76	0.80	0.92	0.84

Notes:

[a] $\bar{y}$ is the average dilution of the corration due to sampling mis-match.

[b] $\sigma_{r'}$ is the estimated error in r' from a ''jackknife'' computation (see text for details).

[c] $t = r^\dagger[(\nu-2)/(1-r^{\dagger 2})]^2$, approximate distribution given by Student's t-distribution.

[d] Probability of rejecting the hypothesis $\rho = 0$.

[e] The effective d.o.f. for the F-$\lvert\alpha\rvert$ correlations have been reduced by 2 to account for the decision to fold and for computing the optimum folding point. Without this reduction, $\nu = 10.2$ (6-day intervals) and 15.4 (4-day intervals).

REFERENCES

Bethea, R. H., Duran, B. S., and Boullion, T. L. 1985, Statistical Methods for Engineers and Scientists, 2nd ed. (New York: M. Dekker).

Boynton, P. E., and Deeter, J. E. 1986, in Proc. of the Workshop on Time Studies of X-ray Sources, ed. S. Hayakawa and F. Nagase (Dept. of Astrophyics, Nagoya Univ.), p. 1.

Boynton, P. E., Deeter, J. E., Lamb, F. K., Zylstra, G., Pravdo, S. H., White, N. E., Wood, K. S., and Yentis, D. J. 1984, Ap. J. (Letters), 283, L53.

Boynton, P.E., Deeter, J. E., Lamb, F. K., and Zylstra, G. 1986, Ap. J., 307, 545.

CRC Handbook of Tables for Probability and Statistics (Second Edition), ed. W. H. Beyer (Cleveland: The Chemical Rubber Company).

Deeter, J. E. 1984, Ap. J., 281, 482.

Deeter, J. E., and Boynton P. E. 1982, Ap. J., 261, 337.

Deeter, J. E., Boynton, P. E., Lamb, F. K., and Zylstra, G. 1989, Ap. J., 336, 376.

Deeter, J. E., Boynton, P. E., Shibazaki, N., Hayakawa, S., Nagase, F., and Sato, N. 1987, A. J., 93, 877.

Efron, B. 1982, The Jackknife, the Bootstrap and Other Resampling Plans (Philadelphia: S.I.A.M.).

Ghosh, P., and Lamb, F. K. 1978 Ap. J. (Letters), 223, L83.

---------. 1979a Ap. J., 232, 259.

---------. 1979b Ap. J., 234, 296.

Green, J. R., and Margerison, D. 1978, Statistical Treatment of Experimental Data (Amsterdam: Elsevier Scientific Publishing Co.).

Lamb, F. K. 1977, in Proc. 8th Texas Symposium on Relativistic Astrophysics (Ann. NY Acad. Sci., 302, 482).

---------. 1985, in Proc. Japan-U.S. Seminar on Galactic and Extragalactic Compact X-ray Sources, ed. Y. Tanaka and W. H. G. Lewin (Tokyo: ISAS).

---------. 1989, in Timing Neutron Stars, ed. H. Ögelman and E. P. J. van den Heuvel (Dordrect: Kluwer Academic Press), in press.

Lamb, F. K., Pines, D., and Shaham, J. 1978a, Ap. J., 224, 969.

---------. 1978b, Ap. J., 225, 582.

Lamb, F. K. et al.1989, in preparation.

Lindgren, B. W. 1962, Statistical Theory (New York: The Macmillian Co.).

Nagase, F. et al. 1982, ISAS Research Note 178 (Tokyo: ISAS).

Nagase, F. et al. 1984, Ap. J., 280, 259.

Parmar, A. N., White, N. E., Stella, L., Izzo, C., and Ferri, P. (1988), Ap. J., in press.

Rappaport, S., and Joss, P. C. 1977, Nature, 266, 683.

van der Klis, M., and Bonnet-Bidaud, J. M. 1984, Astr. Ap., 135, 155.

FIGURE CAPTIONS

Fig. 1. Pulse phase and harmonic phases of the Vela X-1 pulse, as a function of time, based on Hakucho data taken in 1981 January. The horizontal axis is Julian day, minus 2,440,000, and the vertical axis is pulse phase in seconds. The top panel shows the residual pulse phase with respect to a local, constant pulse frequency. The remaining panels, numbered (2) through (6) to indicate the individual harmonic numbers, show the residual harmonic phases with respect to a quadratic fit to the pulse phase. For reference, the pulse period of Vela X-1 is 283 s.

Fig. 2. (a) Power spectrum of the noise in X-ray flux for Vela-X-1, based on the high energy (9--22 keV) channel. The abscissa is the logarithm of analysis frequency in days^{-1}, and the ordinate is logarithm of power density ($\text{cnts}^2\ \text{cm}^{-4}\ \text{s}^{-1}$). (b) Expected power spectrum of the flux noise if it obeyed an f^{-2} power law (white noise in the derivative of the flux).

Fig. 3. (a) Correlation between flux and angular acceleration for Vela X-1, averaged over intervals of 6 days duration. The abscissa is the X-ray flux (9-22 keV), in counts $\text{cm}^{-2}\ \text{s}^{-1}$, corrected to center collimator, and also corrected for a term to remove orbital variation. The ordinate is the average angluar acceleration, in units of rad s^{-2}. (b) Correlation between flux and $|\alpha - \alpha_o|$, with flux and α averaged over the same intervals as in (a). The value $\alpha_o = -2.5 \times 10^{-12}$ rad s^{-2} used in this figure was chosen to maximize the correlation between flux and $|\alpha - \alpha_o|$. The units are the same as for (a), but here the flux has not been correction for orbital variation. (c) Same as (a), except that here the flux and angular (d) Same as (b), here using the 4-day averages.

P. E. Boynton and J. E. Deeter: Department of Astronomy, FM-20, University of Washington, Seattle, WA 98195, U.S.A.

S. Hayakawa: Department of Astrophysics, Faculty of Science, Nagoya University, Chikusa-ku, Nagoya 464, Japan.

F. Nagase: Institute of Space and Astronautical Science, 3-1-1, Yoshinodai, Sagamihara-shi, Kanagawa-ken 229, Japan.

N. Shibazaki: Department of Physics, Rikkyo University, Nishi-Ikebukuro, Toshima-ku, Tokyo 171, Japan.

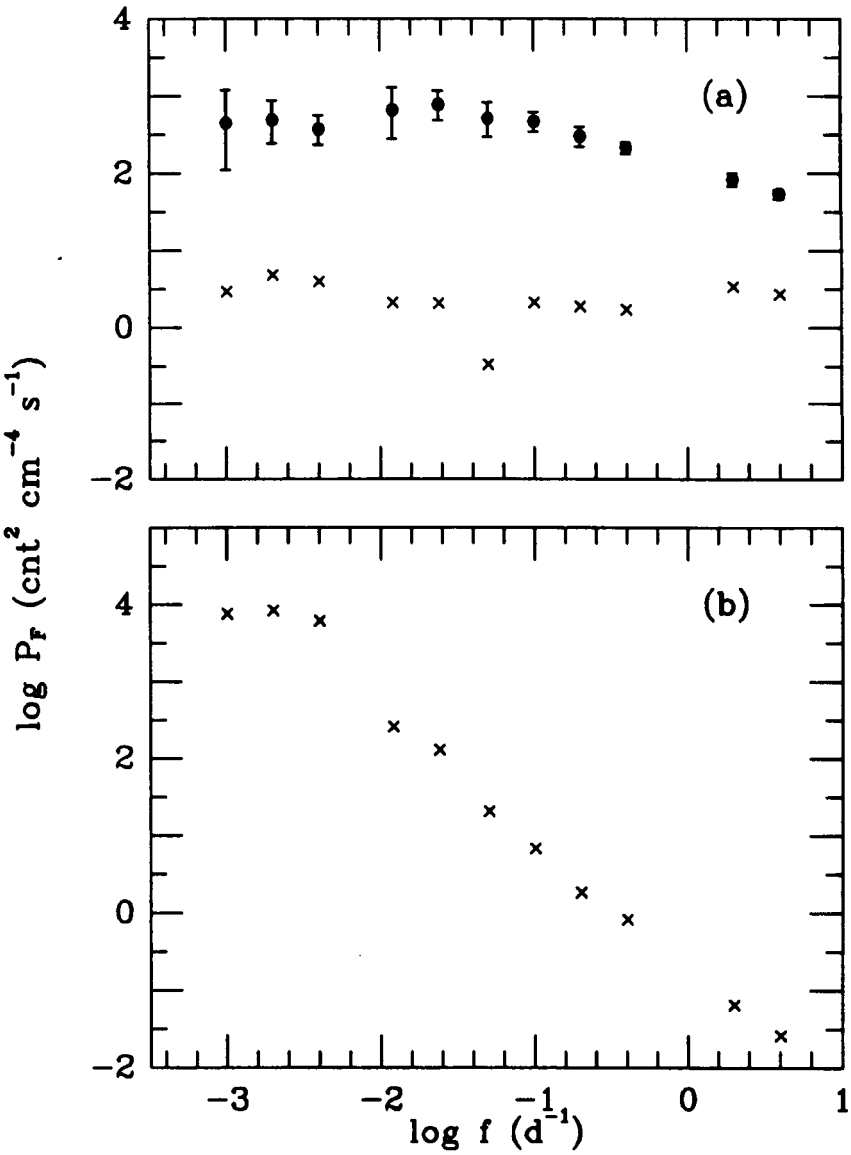

Fig. 1

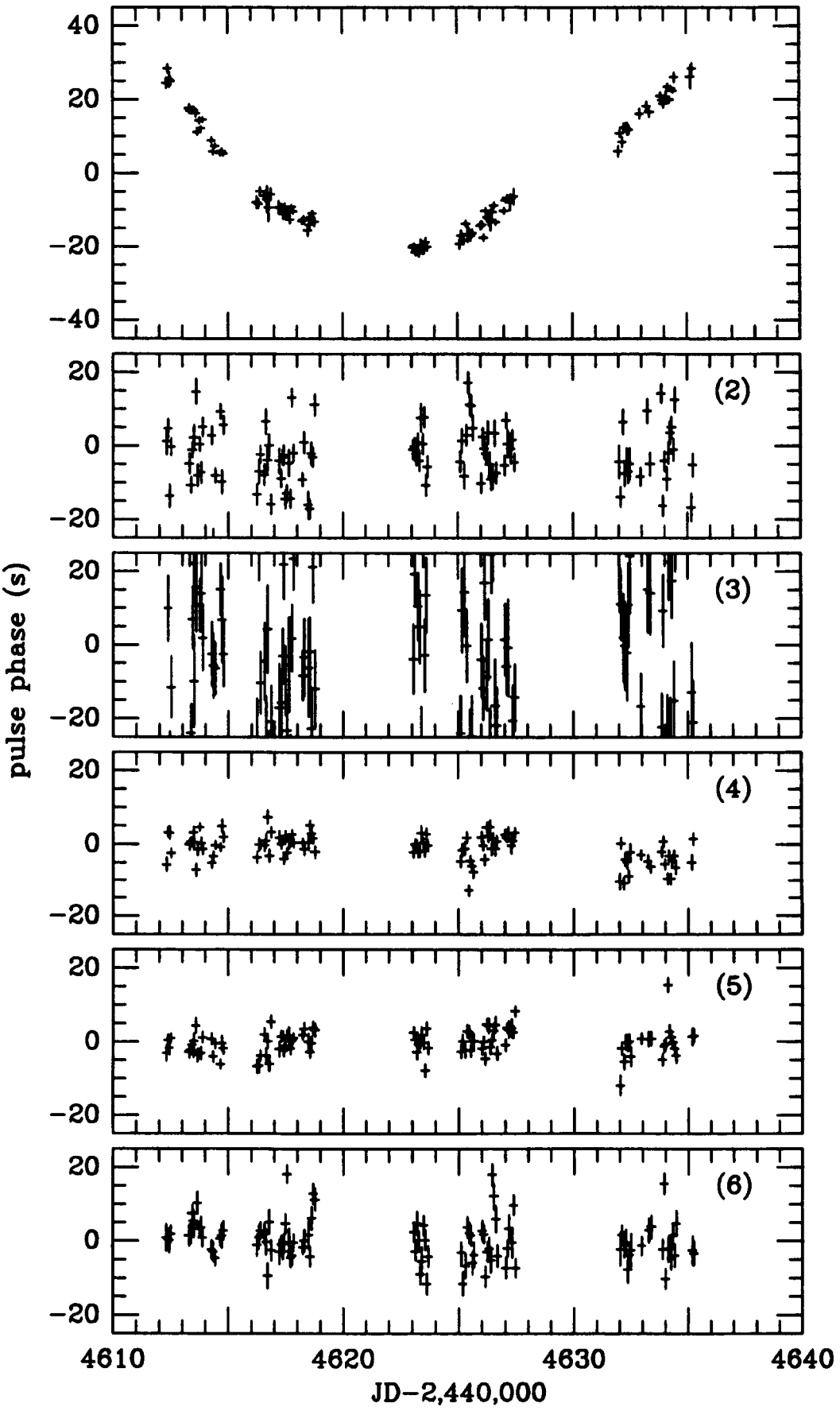
40
20
0
−20
−40
(2)
(3)
(4)
(5)
(6)
pulse phase (s)
4610
4620
4630
4640
JD−2,440,000

Fig. 2

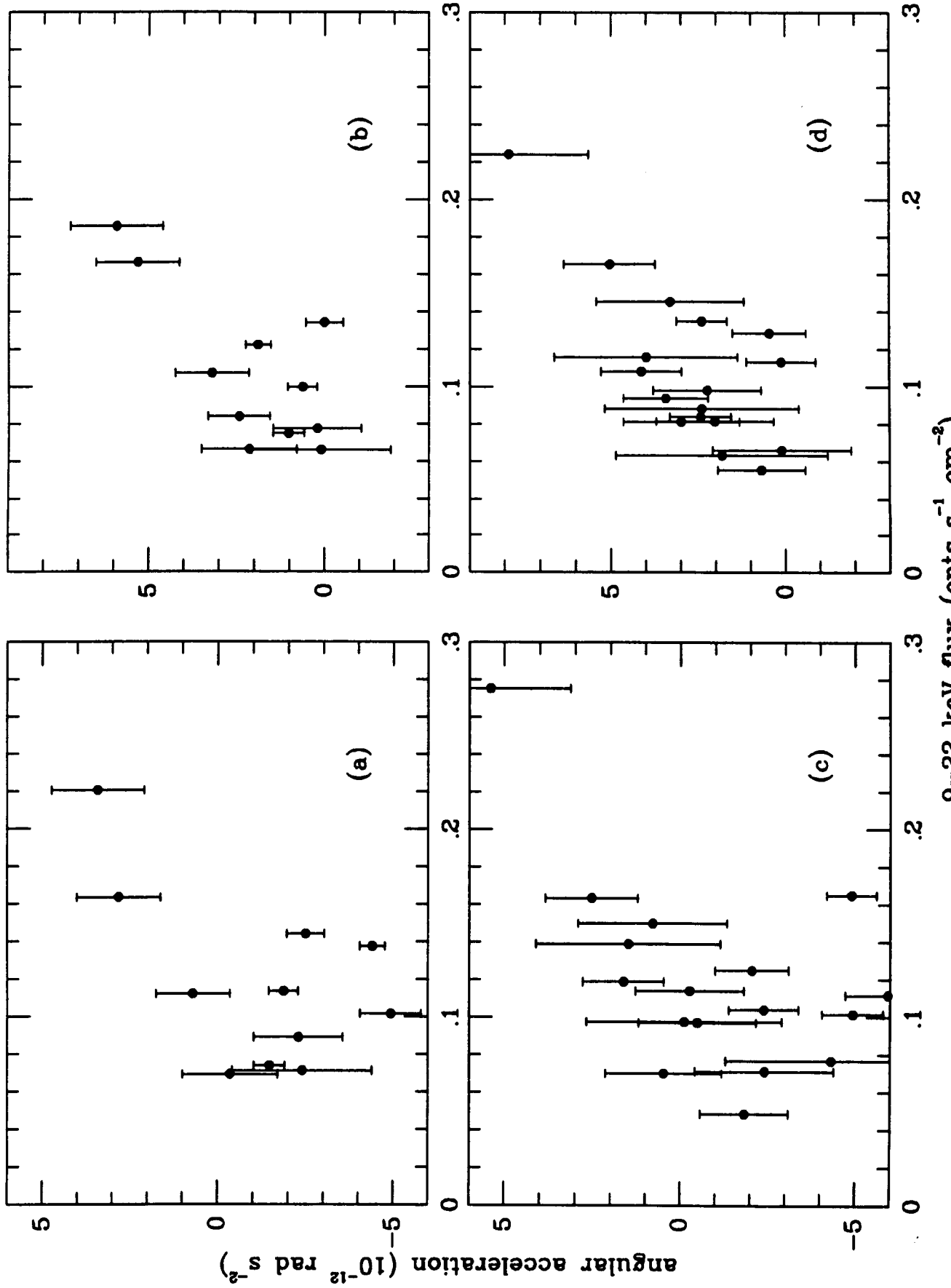
(a)
(b)
(c)
(d)
angular acceleration (10^{-12} rad s^{-2})
9–22 keV flux (cnts s^{-1} cm^{-2})

Fig. 3